Multiple scattering of charged particles in a free-electron gas

Claudio D. Archubi and Néstor R. Arista
División Colisiones Atómicas, Instituto Balseiro and Centro Atómico Bariloche, RA-8400 Bariloche, Argentina
(Received 15 June 2006; published 30 November 2006)

We study the influence of electron-scattering processes on the angular distributions of point particles moving through a free-electron gas. Previous calculations for slow ions are extended to all (nonrelativistic) velocities. The formulation is based on the extension of the multiple-scattering theory to the case of particles moving through a free-electron gas, using Lindhard's dielectric function to separately evaluate the contributions of binary (electron-hole) and collective (plasmon) excitations. We find that the angular spread of the beam of particles is dominated by binary collisions. The results for the width of the angular distribution are compared with an integral expression derived by Lindhard.

DOI: 10.1103/PhysRevA.74.052717 PACS number(s): 34.50.Fa

I. INTRODUCTION

The phenomenon of multiple scattering is one of the relevant processes in the interaction of ionized particles with matter, and in particular, is the process that determines the angular spread of a beam of particles after traversing dense or dilute media. This process has been extensively studied over the years, and the basic theoretical aspects have been described by several authors using various statistical approaches [1–8].

The angular spread of a beam of ions traversing matter is usually dominated by multiple-scattering effects produced by atomic interactions. The electronic contribution to this process is in most cases negligible due to the very small mass ratio between target electrons and incident ions. However, in channeling experiments, where the atomic collisions with crystal atoms are strongly reduced [9,10], multiple scattering by target electrons may produce a notorious contribution and increase the dechanneling fraction. These effects have been taken into account for protons in various crystals [11] and may be expected to be more pronounced in the case of muons or pions [12–14].

In a previous study [15] we have considered the effects of electronic multiple scattering for the case of slow ions in a free-electron gas (representing the conduction or valence electrons in a solid). The purpose of the present work is to extend the previous study to higher energies in order to have a complete characterization of the electronic contribution to the multiple scattering in all ranges, and also, to provide elements for more comprehensive analyses of channeling effects in future studies.

The extended formulation refers to singly charged particles and is based, on one side, on the standard theory of multiple scattering in random media [7,8], and on the other, on the perturbative description provided by the dielectric function formalism [16,17] appropriate to the case of swift particles.

The basic formulation of the momentum-transfer probability in single-scattering theory is described in Sec. II. Calculations showing the contributions of individual and collective excitations are included in this section. Finally, calculations of the angular distributions resulting from the multiple-scattering process are described and analyzed in Sec. III, where we also compare our results with a general expression obtained by Lindhard [16].

II. SINGLE SCATTERING

We start by considering the process of inelastic scattering of an incident ion due to the interaction with the valence electrons of a solid. The electrons will be represented as a free-electron gas with density n_e, Fermi velocity v_F, and one-electron radius r_s (with $4\pi r_s^3/3=1/n_e$ and $v_F=1.919/r_s$ in atomic units).

We formulate the scattering process following the dielectric function formalism. According to Refs. [17,18] the scattering probability for momentum transfer $\hbar\vec{q}$ and energy transfer $\hbar\omega$ may be expressed as

$$\frac{d^4P}{d^3q\,d\omega}=\frac{e^2}{\pi^2q^2}\,\mathrm{Im}\left[\frac{-1}{\varepsilon(q,\omega)}\right]\delta(\hbar\omega-\hbar\vec{q}\cdot\vec{v}), \tag{1}$$

where $\varepsilon(q,\omega)$ denotes the dielectric function and $\vec{v}$ is the ion velocity. We will assume that the energy loss of the ion is sufficiently small (relative to its initial energy) so that the value of v will be kept constant in the calculations.

Following Ref. [15] we first integrate over frequencies ω, and then separate the momentum transfer into parallel ($q_\parallel$) and perpendicular ($q_\perp$) components relative to the initial beam direction, $d^3q=d^2q_\perp dq_\parallel$. Integrating over $q_\parallel$ we get the differential probability of scattering with perpendicular momentum transfer $q_\perp$,

$$\frac{d^2P}{d^2q_\perp}=\int\frac{d^3P}{d^3q}dq_\parallel=\frac{e^2}{\hbar\pi^2}\int\frac{dq_\parallel}{(q_\parallel^2+q_\perp^2)}\,\mathrm{Im}\left[\frac{-1}{\varepsilon(q,\omega)}\right]\Bigg|_{\omega=q_\parallel v}, \tag{2}$$

with the relation $\omega=q_\parallel v$.

This expression yields the probability of scattering of the incident ion and the associated angular deflection in single-scattering events, and includes also the dynamical screening produced by the electron gas.

For the evaluation of Eq. (2) we use the complete expression of Lindhard for the dielectric function [16] in the form

$$\varepsilon(q,\omega) = \varepsilon_1(q,\omega) + i\varepsilon_2(q,\omega), \tag{3}$$

with

$$\varepsilon_1(q,\omega) = 1 + \frac{3\omega_P^2}{q^2 v_F^2} f_1(u,z), \tag{4}$$

$$\varepsilon_2(q,\omega) = \frac{3\omega_P^2}{q^2 v_F^2} f_2(u,z), \tag{5}$$

where

$$f_1(u,z) = \frac{1}{2} + \frac{1}{8z}\{1-(z-u)^2\}\log\left|\frac{z-u+1}{z-u-1}\right| + \frac{1}{8z}\{1-(z+u)^2\}\log\left|\frac{z+u+1}{z+u-1}\right|, \tag{6}$$

$$f_2(u,z) = \begin{cases} \dfrac{\pi}{2}u, & z+u<1 \\ \dfrac{\pi}{8z}\{1-(z-u)^2\}, & |z-u|<1<z+u \\ 0, & |z-u|>1, \end{cases} \tag{7}$$

with $u=\omega/qv_F$ and $z=q/2k_F$.

Due the azimuthal symmetry we may replace $d^2q_\perp = 2\pi q_\perp dq_\perp$ in Eq. (2). Then, after changing the integration variable from $q_\parallel$ to $q=\sqrt{q_\parallel^2+q_\perp^2}$ we obtain

$$\frac{dP}{dq_\perp} \equiv vG(q_\perp,v) = \frac{2e^2}{\pi\hbar} q_\perp \int_{q_\perp}^{q_{\max}} \frac{dq}{q\sqrt{q^2-q_\perp^2}} \operatorname{Im}\left[\frac{-1}{\varepsilon(q,\omega)}\right]\Bigg|_{\omega=\omega_q}, \tag{8}$$

where we introduce the notation $\omega_q = q_\parallel v = v\sqrt{q^2-q_\perp^2}$, which defines an integration line in the (ω,q) plane. The upper limit of integration $q_{\max}$ will be indicated below. This expression defines the function $G(q_\perp,v)$, which depends on the ion velocity v and perpendicular momentum transfer $q_\perp$.

The integral in Eq. (8) extends over the regions in which $\operatorname{Im}\left[\frac{-1}{\varepsilon(q,\omega)}\right] \neq 0$, illustrated in Fig. 1, and contains two contributions: individual and collective excitations, which will be treated separately.

A. First contribution: Individual excitations $[\varepsilon_2(q,\omega)\neq 0]$

The contribution of binary excitations, or electron-hole pairs, is given by the shaded region, where $\varepsilon_2(q,\omega)\neq 0$ [18–20]. The parabolic curves correspond to the two limiting cases implicit in the condition $|z-u|\leq 1$, namely, $\omega_\pm(q) = (v_F/2k_F)q^2 \pm qv_F$ (note that $v_F=k_F$ in atomic units).

The integration over q is performed along the part of the integration line,

$$\omega_q(q,q_\perp) = v\sqrt{q^2-q_\perp^2}, \tag{9}$$

which crosses the shaded region between $\omega_+(q)$ and $\omega_-(q)$ in Fig. 1 (full lines). Two illustrative cases are shown, corresponding to $q_\perp=1$ and $q_\perp=3.5$ (values in atomic units), which provide one contribution ($q_\perp=3.5$) or two separate contributions ($q_\perp=1$) to the function $G_{eh}(q_\perp,v)$ belonging to electron-hole excitations. The *low-q* contribution is comparatively very small (as follows from the numerical calculations) due to the strong screening effects present in this region. The upper limit of the integral in Eq. (8) denoted by $q_{\max}$ is given by the intersection of the curves ω_q and $\omega_-(q)$. It should be noted that the integration line ω_q depends on the three quantities: $q, q_\perp$, and v; note also that if $q_\perp \to 0$ the curve for ω_q becomes a straight line, $\omega_q \to qv$ (line a in the figure).

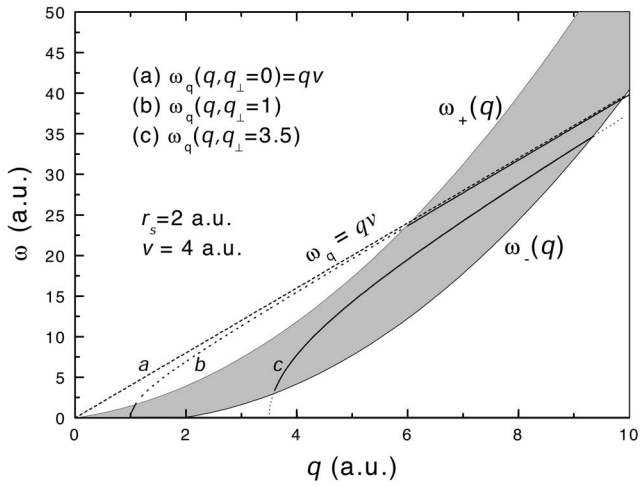

FIG. 1. Regions of integration considered to obtain the probability function $G_{eh}(q_\perp,v)$ for the scattering of protons by individual electrons in a free-electron gas, with transverse momentum transfer $q_\perp$, according to the dielectric formulation for $v=4$ a.u. and $r_s=2$ a.u. The dashed region between the curves ω_+ and ω_- indicates the range of individual excitations, where $\varepsilon_2(q,\omega)\neq 0$. The lines a,b,c show different lines of integration, given by $\omega_q = v\sqrt{q^2-q_\perp^2}$, corresponding to three fixed values of $q_\perp$. The straight line (a) $\omega = qv$ corresponds to the case $q_\perp=0$, while the curves (b) and (c) correspond to $q_\perp=1$ a.u. and $q_\perp=3.5$ a.u., respectively.

B. Second contribution: Plasmon excitations $[\varepsilon(q,\omega)=0]$

To analyze the plasmon contribution it is necessary to determine first the resonance line, corresponding to the solutions of $\varepsilon_1(q,\omega)=0$ in the region where $\varepsilon_2(q,\omega)=0$, that is, $f_1(u,z) = \frac{-q^2v_F^2}{3\omega_P^2}$. The solution of this equation was determined numerically using Eq. (6). It yields a dispersion relation for plasmons, which may be alternatively denoted by $\omega=\omega_r(q)$ or $q=q_r(\omega)$.

Since the plasmon line has the property of a Dirac's delta function the integral in Eq. (8) reduces now to a single value. To determine this value we expand the energy-loss function around the resonance line and obtain formally the expression

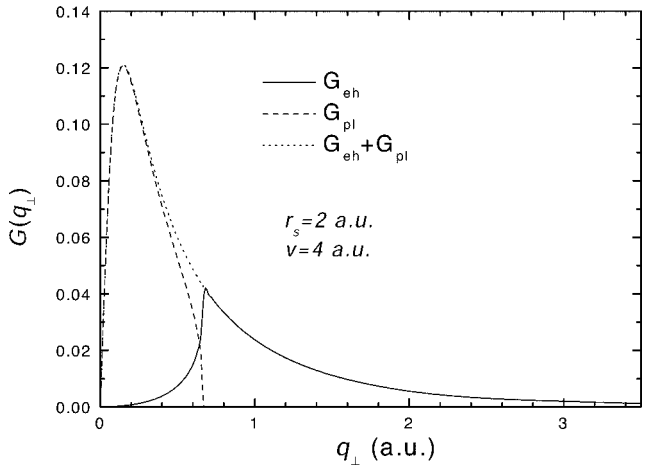

FIG. 2. Comparison between the functions $G_{eh}(q_\perp,v)$ for the scattering of protons with individual electrons, and $G_{pl}(q_\perp,v)$ for the scattering of protons with plasmons in a free-electron gas, as a function of the transverse momentum transfer $q_\perp$ for $r_s=2$ a.u. and $v=4$ a.u. Note that at the point $q_\perp^{pl\text{-max}}=0.66$, where the plasmon term vanishes (in this particular example), the electron-hole term shows a critical (cusp) behavior.

$$\mathrm{Im}\left[\frac{-1}{\varepsilon(q,\omega_q(q,q_\perp))}\right]\Bigg|_{\mathrm{pl}} = \left[\frac{\varepsilon_2}{\varepsilon_1^2+\varepsilon_2^2}\right]\Bigg|_{\varepsilon_2\to 0} = \pi\delta[\varepsilon_1(q,\omega_q(q,q_\perp))] = \frac{\pi}{|\varepsilon_1'[q_r]|}\delta(q-q_r), \tag{10}$$

where

$$\varepsilon_1'[q_r] = \frac{\partial}{\partial q}\varepsilon_1(q,\omega_q(q,q_\perp)) + \frac{\partial}{\partial\omega_q}\varepsilon_1(q,\omega_q(q,q_\perp))\frac{qv}{\sqrt{q^2-q_\perp^2}}\Bigg|_{q=q_r}, \tag{11}$$

with q_r determined by

$$\varepsilon_1(q_r,\omega_q(q_r,q_\perp))=0, \tag{12}$$

which corresponds to the intersection of the plasmon resonance line $\omega_r(q)$ with the integration line $\omega_q(q,q_\perp)$ of Eq. (9).

To find the contribution of plasmons to the scattering probability we use the integral expression of Eq. (8). Because of the delta behavior of Eq. (10) the full contribution to the integral is given by a single point (q_r,ω_r) in the (q,ω) plane for each value of $q_\perp$. Thus, the corresponding expression for the probability is finally given by

$$G_{pl}(q_\perp,v)=\frac{1}{v}\frac{dP}{dq_\perp}=\frac{2e^2q_\perp}{\hbar v q_r\sqrt{q_r^2-q_\perp^2}}\frac{1}{|\varepsilon_1'[q_r]|}, \tag{13}$$

where the value of q_r is determined by Eq. (12) (note that q_r is a function of v and $q_\perp$).

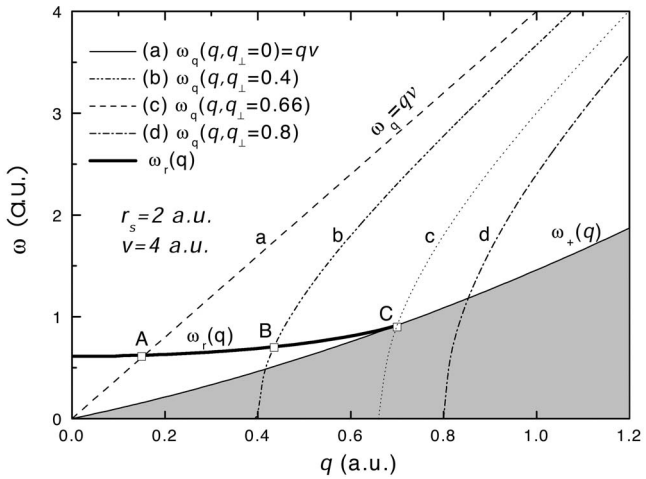

FIG. 3. Region of integration to obtain the plasmon contribution to the probability function $G_{pl}(q_\perp,v)$ for three illustrative values of $q_\perp$ (0, 0.4, and 0.66). The broad solid line ω_r is the plasmon resonance line. As explained in the text the plasmon contribution is concentrated in the crossing points, indicated by A,B,C, for the three assumed values of $q_\perp$. Curve (d) shows a case with $q_\perp > q_\perp^{pl\text{-max}}$ where there is no plasmon contribution.

The resulting functions $G_{eh}(q_\perp,v)$ and $G_{pl}(q_\perp,v)$, corresponding to electron-hole and plasmon excitations, are depicted in Fig. 2, for the example of $v=4$ a.u. and $r_s=2$ a.u. For high velocities, the plasmon contribution is important in the range of low $q_\perp$, whereas binary excitations dominate the high-$q_\perp$ region. This is in accordance with the usual physical picture of the relative significance of each type of excitations [19]. It should be noted that the $q_\perp^{\max}$ value for plasmon excitation coincides with the critical point in the spectrum of binary excitations, as observed in Fig. 2.

In order to understand the dependence of $G_{eh}(q_\perp,v)$ and $G_{pl}(q_\perp,v)$ on $q_\perp$, its origin is discussed within the ω-q plot in Fig. 3. We show the plasmon line together with typical integration lines $\omega_q(q,q_\perp)$ [Eq. (9)], for a velocity $v=4$ a.u. and four values of $q_\perp$. The intersection point C corresponds to the critical values (q_c,ω_c) and in this particular case yields $q_\perp=q_\perp^{pl\text{-max}}=0.66$. This corresponds to the maximum perpendicular momentum transfer in plasmon excitation, so that for $q_\perp > q_\perp^{pl\text{-max}}$ (like case d in Fig. 3) the plasmon contribution vanishes. Taking into account that $\mathrm{Im}(-1/\varepsilon)$ has a peak at the critical point C and decreases with increasing distance from this point, it follows that $G_{eh}(q_\perp,v)$ has a maximum at $q_\perp=0.66$, while G_{pl} is the dominating contribution for $q_\perp < q_\perp^{pl\text{-max}}=0.66$, as illustrated in Fig. 2.

With respect to the contribution of plasmon excitations, since $G_{pl}(q_\perp,v)=0$ for $q_\perp > q_\perp^{pl\text{-max}}$, it follows that there is a critical velocity, $v_{crit}=\omega_c/q_c$, so that $G_{pl}\equiv 0$ for $v<v_{crit}$ [because there is no intersection of $\omega_q(q,q_\perp)$ with $\omega_r(q)$, for any $q_\perp$, if $v<v_{crit}$]. This is of course a consequence of the existence of a well-defined threshold for plasmon excitation in Lindhard's theory.

III. MULTIPLE SCATTERING

Following the formulation of Ref. [15] (see also Ref. [8]) we express the electronic multiple-scattering (EMS) function in the small-angle approximation by

$$f(\alpha,x) = \int_0^\infty \kappa d\kappa J_0(\kappa\alpha)\exp[-x\mu_0(\kappa)]. \quad (14)$$

The function $\mu_0(\kappa)$ is determined from the previously defined scattering function $G(q_\perp,v)$ for the present case of an electron gas, by

$$\mu_0(\kappa) = n_e \int [1 - J_0(\kappa\psi_{ion})]d\sigma = \int_0^{2k_F} [1 - J_0(\kappa q_\perp \hbar/M_1 v)]G(q_\perp,v)dq_\perp, \quad (15)$$

with $\psi_{ion}=\hbar q_\perp/M_1 v$, being M_1 the ion mass, and where the differential cross section $d\sigma$ is given by

$$d\sigma = \frac{1}{n_e v}dP = \frac{1}{n_e}G(q_\perp,v)dq_\perp, \quad (16)$$

where we used the relation between the momentum transfer $q_\perp$ and the ion angular deflection ψ_{ion} in the small-angle approximation, namely, $\hbar q_\perp = M_1 v \psi_{ion}$.

We have calculated the multiple-scattering angular distribution according to Eqs. (14)–(16) using the values of $G(q_\perp,v)$ for the electron-hole and plasmon excitations calculated previously, and considering the three alternatives: electron hole contribution (eh), plasmon contribution (pl), and the sum of both $[G_{total}(q_\perp,v)=G_{eh}(q_\perp,v)+G_{pl}(q_\perp,v)]$. Our results show that the angular distribution $f(\alpha,x)$ is dominated by electron-hole excitations, and is well represented by a Gaussian function with an angular width $\alpha_{1/2}$, defined by $f(\alpha_{1/2},x)/f(0,x)=0.5$, which is therefore the relevant quantity of interest to characterize the EMS distribution.

The differences between the results of $\alpha_{1/2}$ corresponding to binary excitations and the total (plasmon plus binary) are always very small, showing the relatively small contribution of plasmons to the total effect. Additionally, we find that the angular spread follows in a good approximation a simple dependence with the square root of the target thickness, $\alpha_{1/2} \cong c\sqrt{x}$.

The small contribution of plasmons to the total width shows an interesting contrast between energy loss and multiple-scattering terms, since, as is well known, plasmon excitation yields a significant fraction of the total stopping power at high energies (partition rule [19]). We can understand this difference by noting that individual and collective contributions add up linearly in the energy loss but quadratically in the angular dispersion, being this dominated by the higher-momentum transfers involved in binary collisions, as illustrated in Fig. 2.

The results for the width of the EMS distribution are shown in Fig. 4, for two typical values of r_s (r_s=1.5 a.u. and r_s=2 a.u.). We have chosen a typical target thickness x =800 a.u. (values for other thicknesses may be obtained by using the square-root dependence of $\alpha_{1/2}$). The solid and open symbols in this figure are the results including only electron-hole pairs and the total contribution (electron-hole and plasmons). The up and down triangles shown at low energies (for both r_s values) are the results obtained from our previous calculations following a nonlinear approach [15],

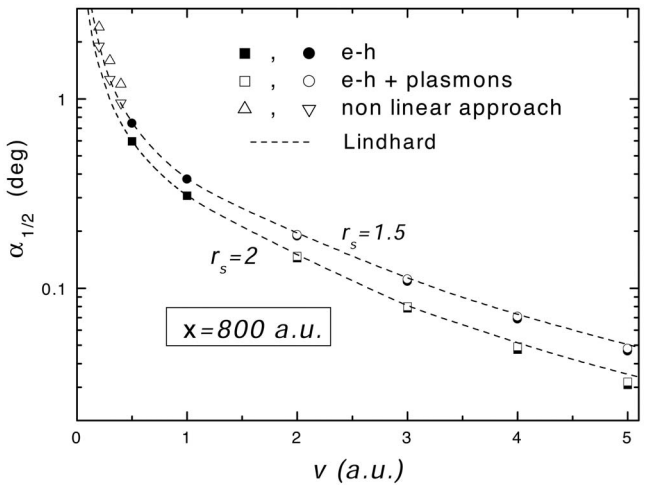

FIG. 4. Comparison between the values of $\alpha_{1/2}$ for protons traversing an 800 a.u. foil, including only individual excitations (solid symbols) and adding plasmon contribution (open symbols) for r_s =1.5 a.u. and r_s=2 a.u., as indicated. The dashed lines show the values obtained using Lindhard's relation, Eq. (17). For comparison, we also include the low-velocity results from Ref. [15] obtained from a non-linear formulation (appropriate for slow ions).

which yields a more accurate description for low energies.

The present results can be compared with the values of $\alpha_{1/2}$ obtained using Lindhard's formula, Eq. (4.19) in Ref. [16], applied here to protons, namely,

$$\alpha_{1/2} = [\ln 2\langle\delta\Phi^2\rangle]^{1/2} = \frac{\sqrt{x\ln 2}}{M_1 v^2}\left\{\frac{\hbar e^2}{\pi}\,\mathrm{Im}\left[2\int_0^\infty \frac{dq}{q}\int_0^{qv} d\omega \frac{\omega^2/v^2 - q^2}{\varepsilon(q,\omega)}\right]\right\}^{1/2}, \quad (17)$$

where M_1 is the proton mass and all quantities are given here in absolute units. The calculations shown here were provided by Gärtner [21], and were also reproduced by our own calculations using the dielectric function of Eqs. (3)–(7) by direct integration in the ω-q plane. We find a remarkable agreement of the Lindhard's prediction (dashed lines in Fig. 4) with the full calculations produced by the multiple-scattering formalism in the linear approximation.

The use of a linear approach is well established for swift particles ($v \gg v_F$). Hence the present calculations would be more accurate at high energies. Conversely, in the low-energy range, our previous calculations [15] based on a nonlinear treatment of the interactions would be more appropriate. The transition from high to low energies is relatively smooth, as Fig. 4 indicates, so that in practice an interpolation procedure may be fully adequate.

In summary, we have investigated the influence of electronic-scattering processes on the angular dispersion of atomic projectiles moving through a free-electron gas. We

have performed numerical calculations based on the general multiple-scattering theory, using the dielectric function approach to represent the dynamical interactions. The angular widths of the distributions obtained from these calculations are in excellent agreement with a previous expression derived by Lindhard and apply in the range of velocities larger than the Fermi velocity.

ACKNOWLEDGMENTS

The authors are grateful to Dr. K. Gärtner for kindly providing the results of numerical calculations indicated in the text and for a careful review of the manuscript. This work has been partially supported by ANPCYT, Argentina (Grant No. PICT-R00122/02). C.D.A. wishes to thank the CONICET.

[1] W. Bothe, Z. Phys. **5**, 63 (1921).
[2] S. Goudsmit and J. L. Saunderson, Phys. Rev. **57**, 24 (1940); Phys. Rev. **58**, 36 (1940).
[3] G. Molière, Z. Naturforsch. A **3a**, 78 (1948).
[4] H. S. Snyder and W. T. Scott, Phys. Rev. **76**, 220 (1949).
[5] H. Bethe, Phys. Rev. **89**, 1256 (1953).
[6] W. T. Scott, Rev. Mod. Phys. **35**, 231 (1963).
[7] L. Meyer, Phys. Status Solidi B **44**, 253 (1971).
[8] P. Sigmund and K. B. Winterbon, Nucl. Instrum. Methods **119**, 541 (1974).
[9] D. S. Gemmell, Rev. Mod. Phys. **46**, 129 (1974).
[10] J. Lindhard, K. Dan. Vidensk. Selsk. Mat. Fys. Medd. **34**, No. 14, 1 (1965).
[11] K. Gärtner, K. Hehl, and G. Schlotzhauer, Nucl. Instrum. Methods Phys. Res. **216**, 275 (1983).
[12] B. D. Patterson, Rev. Mod. Phys. **60**, 69 (1988).
[13] G. Flik *et al.*, Phys. Rev. Lett. **57**, 563 (1986).
[14] J. E. Valdés, P. Vargas, and N. R. Arista, Phys. Rev. Lett. **85**, 4731 (2000).
[15] C. D. Archubi and N. R. Arista, Phys. Rev. A **72**, 062712 (2005).
[16] J. Lindhard, K. Dan. Vidensk. Selsk. Mat. Fys. Medd. **28**, No. 8, 1 (1954).
[17] R. H. Ritchie, Phys. Rev. **114**, 644 (1959).
[18] D. Pines, *Elementary Excitations in Solids* (Benjamin, New York, 1963).
[19] J. Lindhard and A. Winther, K. Dan. Vidensk. Selsk. Mat. Fys. Medd. **34**, 1 (1964).
[20] N. R. Arista, Phys. Rev. B **18**, 1 (1978).
[21] K. Gärtner (private communication).